Integer Frequency Offset Detection Methods for OFDM-Based WLAN Systems

Sanghun Kim
School of Information and Communication Engineering, Sungkyunkwan University, Korea.

Sangho Ahn
School of Information and Communication Engineering, Sungkyunkwan University, Korea.

Seung Hwan Yoo
Department of Electronics Engineering, Konkuk University, Korea.

Sun Yong Kim
Department of Electronics Engineering, Konkuk University, Korea.

Seokho Yoon
School of Information and Communication Engineering, Sungkyunkwan University, Korea.
Corresponding author
syoon@skku.edu

ABSTRACT

Recently, a frequency offset estimation method for orthogonal frequency division multiplexing (OFDM) has been proposed by Ren et al. (REA) [9]. The method can estimate an frequency offset for any training symbol structure. In the REA method, however, the integer frequency offset detection probability is rapidly varying according to the fractional frequency offset.

In this paper, we first analyze the REA frequency offset estimation method, and define new detection criteria suitable for integer frequency offset detection. Then, we propose two efficient integer frequency offset estimation methods based on maximum likelihood method. The proposed methods overcome the drawback of the REA method, maintaining its advantage. The numerical results demonstrate that the proposed methods outperform the REA method in terms of the integer frequency offset detection probability.

Keywords

OFDM, integer frequency offset, estimation, training symbol

1. INTRODUCTION

Compared with the conventional single carrier systems, the orthogonal frequency division multiplexing (OFDM) systems provide many advantages, such as robustness to multipath fading, simple equalizer structure, and high efficiency in frequency use [1]. Because of these advantages, the OFDM has already been adopted as the modulation method for standards in communication areas, such as digital subscriber line (DSL), European digital audio and video broadcasting (DAB/DVB), IEEE 802.11a, and European HiperLAN II for wireless local area network (WLAN). Furthermore, recently a multi-user version of the OFDM has been adopted for IEEE standard 802.16 [2].

Permission to make digital or hard copies of all or part of this work for personal or classroom use is granted without fee provided that copies are not made or distributed for profit or commercial advantage and that copies bear this notice and the full citation on the first page. To copy otherwise, to republish, to post on servers or to redistribute to lists, requires prior specific permission and/or a fee.

The OFDM systems, however, are very sensitive to frequency offset (FO) caused by the mismatch of the oscillators in the transmitter and receiver or the Doppler shift. The FO could bring on the inter-carrier interference (ICI) and destroy orthogonality among subcarriers [3], resulting in significant performance degradation. The FO estimation is one of the most important steps for the OFDM receiver. To estimate the FO, various methods based on a training symbol have been investigated [4]-[8].

Moose present maximum likelihood (ML) FO estimation method based on the two consecutive and identical training symbols [4]. The maximum offset that can be estimated in Moose's method is half of the subcarrier spacing. Schmidl and Cox (SC) present FO estimation method using a training symbol that has two identical halves [5]. The maximum FO estimation range of SC method is equal to the subcarrier spacing. Morelli and Mengali (MM) improved the SC method with the best linear unbiased estimation (BLUE) principle. The MM method uses a training symbol composed of multiple identical parts and its FO estimation performance is quite close to the Cramer-Rao lower bound. Kim et al. present the FO estimation method using the relationship among subcarriers in the training symbol [7], whereas the methods [4]-[6] using the relationship among time samples in the training symbol. Laourin et al. (LEA) present an efficient FO estimation method and new training symbol that has phase difference in samples [8]. The LEA method offers a wide FO estimation range with reduced computational complexity. In these [4]-[8] methods, an FO estimation process is dependent on training symbol structure. In other words, the methods in [4]-[8] are necessary specific training symbol structure for FO estimation.

Recently, a generalized FO estimation method has been developed by Ren et al. (REA) [9]. The REA method can estimate an FO independently from training symbol structure, and has an estimation range of overall signal bandwidth without loss of accuracy. In the REA method, the training symbol can be designed for the channel estimation, the timing synchronization, or something else, since it does not requires specific design of training symbol for FO estimation. However, the REA method has the problem that the detection probability of integer frequency offset (IFO) is varying according to fractional frequency offset (FFO).

In this paper, we first define new detection criteria suitable for IFO detection, and then propose two novel IFO detection methods based on the new IFO detection criteria. The proposed methods still have the advantages of REA method, while overcome the drawback. Consequently, frequency estimation performance can be improved by using the proposed methods.

This paper is organized as follows. Section 2 describes the OFDM signal model and conventional REA FO estimation method. In Section 3, we define new detection criteria and propose two novel IFO estimation methods. The simulation results are presented in Section 4. Finally, Section 5 concludes this paper.

2. SIGNAL MODEL AND CONVENTIONAL METHOD

2.1 Signal Model

The nth OFDM sample x_n is generated by the inverse fast Fourier transform (IFFT), and can be expressed as

$$x_n = \frac{1}{\sqrt{N}} \sum_{k=0}^{N-1} X_k e^{j2\pi kn/N}, \text{ for } n = 0, 1, \cdots, N-1, \quad (1)$$

where X_k is a phase shift keying (PSK) or quadrature amplitude modulation (QAM) symbol in the kth subcarrier and N is the size of the IFFT.

Assuming that the timing synchronization is perfect, we can express the nth received OFDM sample y_n as

$$y_n = \sum_{l=0}^{L-1} h_l x_{n-l} e^{j2\pi\varepsilon n/N} + w_n, \text{ for } n = 0, 1, \cdots, N-1, \quad (2)$$

where ε represents the FO normalized to the subcarrier spacing, h_l is the l-th tap coefficient of channel impulse response with the length of L, and w_n is the complex additive white Gaussian noise (AWGN) sample with zero mean and variance σ_n^2. The signal to noise ratio (SNR) is defined as σ_s^2/σ_n^2, where $\sigma_s^2 = E\{|x_k|^2\}$ with $E\{\cdot\}$ denoting the statistical expectation.

For the sake of simple description, the FO ε can be divided into an integer and a fractional parts, i.e.,

$$\varepsilon = \varepsilon_I + \varepsilon_F, \quad (3)$$

where ε_I and $\varepsilon_F \in [0, 1)$ denote the integer and fractional parts of ε, respectively.

2.2 Conventional Method

In REA method, an FO estimate $\hat{\varepsilon}$ can be obtained via the following three estimation steps: integer, fractional, and residual frequency offset (RFO) estimation, i.e.,

$$\hat{\varepsilon} = \hat{\varepsilon}_I + \hat{\varepsilon}_F + \hat{\varepsilon}_R, \quad (4)$$

where $\hat{\varepsilon}_I$, $\hat{\varepsilon}_F$, and $\hat{\varepsilon}_R$ represent the integer, fractional, and residual parts of $\hat{\varepsilon}$, respectively.

In order to make the received training symbol independent from its structure, the envelope equalized processing (EEP) factor f_x is used [9], which is defined as

$$f_x = \frac{x_n^*}{|x_n|^2}. \quad (5)$$

where * denotes the complex conjugate of a complex number.

The received signal equalized by the EEP factor can be expressed as

$$\begin{aligned} y_n^{'} &= y_n f_x \\ &= h_0 x_k e^{j2\pi\epsilon k/N} f_x + \sum_{l=1}^{L-1} h_l x_{n-l} f_x + w_n f_x \\ &= h_0 e^{j2\pi\epsilon k/N} + w_n^{'}, \end{aligned} \quad (6)$$

where $w_n^{'} = \sum_{l=1}^{L-1} h_l x_{n-l} f_x + w_n f_x$, which can be approximated as a zero mean Gaussian random variable by the central limit theorem [10].

In order to estimate the IFO, the following metric is used.

$$\hat{\varepsilon}_I = \arg\max_{\tilde{\varepsilon}_I} \{|R(\tilde{\varepsilon}_I)|^2 + |R(\tilde{\varepsilon}_{I+1})|^2\}, \quad (7)$$

where $\tilde{\varepsilon}_I \in \{-N/2, \cdots, 0, \cdots, N/2\}$ is a trial value of ε_I, and

$$R(\tilde{\varepsilon}_I) = \sum_{n=0}^{N-1} y_n^{'} e^{-j2\pi\tilde{\varepsilon}_I n/N}. \quad (8)$$

The FFO is estimated by

$$\hat{\varepsilon}_F = \frac{|R(\hat{\varepsilon}_I + 1)|}{|R(\hat{\varepsilon}_I)| + |R(\hat{\varepsilon}_I + 1)|}, \quad (9)$$

and the RFO is estimated by

$$\hat{\varepsilon}_R = \frac{|R(\hat{\varepsilon_I} + \hat{\varepsilon}_F + 0.5)| - |R(\hat{\varepsilon}_I + \hat{\varepsilon}_F - 0.5)|}{2\{|R(\hat{\varepsilon}_I + \hat{\varepsilon}_F + 0.5)| + |R(\hat{\varepsilon}_I + \hat{\varepsilon}_F - 0.5)|\}}. \quad (10)$$

From (9) and (10), we can clearly observe that the accuracy of $\hat{\varepsilon}_F$ and $\hat{\varepsilon}_R$ depends on that of $\hat{\varepsilon}_I$, and therefore, it is necessary that the IFO estimator gives accurate results.

3. PROPOSED METHOD

3.1 New Detection Criteria

If we ignore the noise term $w_n^{'}$ in (8), $R(\tilde{\varepsilon}_I)$ can be rewritten as

$$\begin{aligned} R(\tilde{\varepsilon}_I) &\approx \sum_{n=0}^{N-1} h_0 e^{j\pi(\tilde{\varepsilon}_I - \varepsilon)(N-1)/N} \frac{\sin\{\pi(\tilde{\varepsilon}_I - \varepsilon)\}}{\sin\{\pi(\tilde{\varepsilon}_I - \varepsilon)/N\}} \\ &= N h_0 \mathrm{sinc}\{\pi(\tilde{\varepsilon}_\mathrm{I} - \varepsilon)\}, \end{aligned} \quad (11)$$

where $\mathrm{sinc}(x) \triangleq \sin(\pi x)/\pi x$.

From (9), (10), and (11), we get

$$\hat{\varepsilon}_F = \frac{|\mathrm{sinc}(\hat{\varepsilon}_I - \varepsilon + 1)|}{|\mathrm{sinc}(\hat{\varepsilon}_I - \varepsilon)| + |\mathrm{sinc}(\hat{\varepsilon}_I - \varepsilon + 1)|}, \quad (12)$$

and

$$\hat{\varepsilon}_R = \frac{|\mathrm{sinc}(\hat{\varepsilon}_I + \hat{\varepsilon}_F - \varepsilon + 0.5)| - |\mathrm{sinc}(\hat{\varepsilon}_I + \hat{\varepsilon}_F - \varepsilon - 0.5)|}{2\{|\mathrm{sinc}(\hat{\varepsilon}_I + \hat{\varepsilon}_F - \varepsilon + 0.5)| + |\mathrm{sinc}(\hat{\varepsilon}_I + \hat{\varepsilon}_F - \varepsilon - 0.5)|\}}. \quad (13)$$

Figs. 1(a) and 1(b) show $\hat{\varepsilon}_F$ as a function of $\varepsilon - \hat{\varepsilon}_I$ and $\hat{\varepsilon}_R$ as a function of $\varepsilon - \hat{\varepsilon}_I - \hat{\varepsilon}_F$, respectively. As we can see from the figures, $\hat{\varepsilon}_F$ is a linear unbiased estimate in the range of $\varepsilon - \hat{\varepsilon}_I \in [0, 1]$ only, and $\hat{\varepsilon}_R$ in the range of $\varepsilon - \hat{\varepsilon}_I - \hat{\varepsilon}_F \in [-0.5, 0.5]$ only.

Fig. 1(c) shows $\hat{\varepsilon}_R$ as a function of $\varepsilon - \hat{\varepsilon}_I$, which can be obtained by applying the result of (12) to the (13). From the figure, we can see that $\hat{\varepsilon}_R$ is a linear unbiased estimate only in the range of $\hat{\varepsilon}_I \in (\varepsilon - 1.31, \varepsilon + 0.31)$ (-1.31 and 0.31 were rounded off to three decimal places).

Therefore, in accordance with these ranges, it is obvious that the correct FFO estimate $\hat{\varepsilon}_F$ can be obtained only in the range of

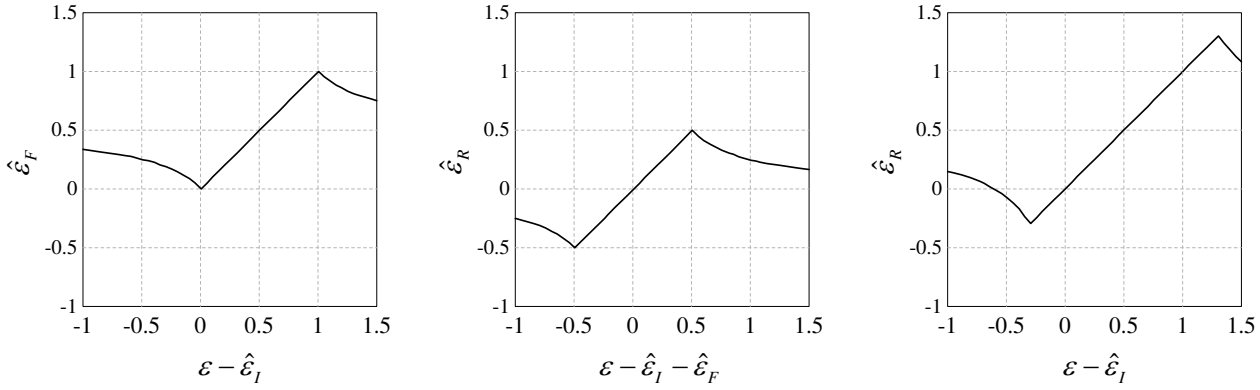

(a) $\hat{\varepsilon}_F$ according to $\hat{\varepsilon}_I - \varepsilon$ (b) $\hat{\varepsilon}_R$ according to $\hat{\varepsilon}_I + \hat{\varepsilon}_F - \varepsilon$ (c) $\hat{\varepsilon}_F + \hat{\varepsilon}_R$ according to $\hat{\varepsilon} + \varepsilon_I$

Figure 1: FFO and RFO estimation metric outputs

$\hat{\varepsilon}_I \in [\varepsilon - 1, \varepsilon]$ and the correct RFO estimate $\hat{\varepsilon}_R$ can be obtained only in the range of $\hat{\varepsilon}_I \in (\varepsilon - 1.31, \varepsilon + 0.31)$.

Conventional methods have been regarded the detection problem as a binary hypothesis problem based on single detection criterion [11]; however, the problem dealt in this paper is not suitable with single detection criterion. The reason is that the ranges can be allowed in FFO and RFO estimation processes are different, and also, there are exists performance disparities between them. Therefore, we define new IFO detection criteria based on these ranges, which are *strict detection criterion* (SDC) and *tolerable detection criterion* (TDC).

Definition 1. Strict detection criterion: An estimate $\hat{\varepsilon}_I$ is a strictly detected at $\hat{\varepsilon}_I \in [\varepsilon - 1, \varepsilon]$.

Definition 2. Tolerable detection criterion: An estimate $\hat{\varepsilon}_I$ is a tolerably detected at $\hat{\varepsilon}_I \in (\varepsilon - 1.31, \varepsilon - 1)$ or $\hat{\varepsilon}_I \in (\varepsilon, \varepsilon + 0.31)$.

If the SDC was satisfied, both FFO and RFO estimation matric can provide unbiased estimates. However, if the TDC was satisfied, FFO estimator can only help the RFO (i.e., strict detected (SD) case gives two repeated estimates, whereas tolerably detected (TD) case gives only one estimate). Hence, in the SD case, we can obtain more accurate results than TD case.

Fig. 2. shows the new detection criteria and REA IFO estimator (7) in the absence of noise. As we can see from the figure that (7) has considerably large values at the outside of SDC and TDC, which can be the cause of the miss detection.

Furthermore, the values of (7) in SDC and TDC are almost same. Since the SD estimate gives more accurate results than TD estimate at the final estimation, therefore, SD is more desired than TD. However, (7) has high probability of selecting a value in the TDC instead of that in the SDC.

3.2 Novel IFO Estimation Method

It is proved in [12] that maximum likelihood (ML) FO estimation metric for ε_I is

$$\hat{\varepsilon}_I = \arg\max_{\tilde{\varepsilon}_I} |R(\tilde{\varepsilon}_I)|^2. \tag{14}$$

When we observe (14) and the previously defined SDC, maxima in (14) does not match with SDC as shown in Fig. 3. On the other hand, the frequency shifted version of (14) gives outstanding matching.

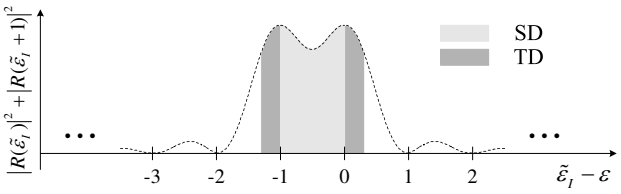

Figure 2: New detection criteria and REA IFO estimation metric

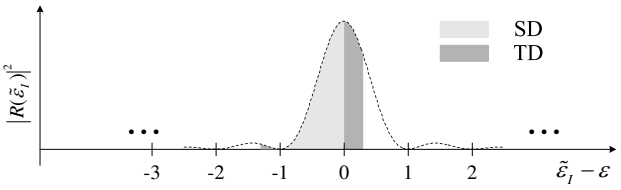

Figure 3: New detection criteria and ML estimation metric

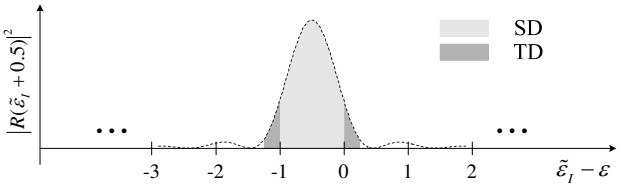

Figure 4: New detection criteria and proposed IFO estimation metric I

Consequently, we propose a first IFO estimation metric as:

$$\hat{\varepsilon}_I = \arg\max_{\tilde{\varepsilon}_I} |R(\tilde{\varepsilon}_I + 0.5)|^2, \tag{15}$$

which is shown in Fig. 4. As we can see from the figure, the proposed IFO estimation metric I does not give large values at the outside of SDC and TDC regions, and also has large difference between SDC and TDC compared with (7). Consequently, the proposed IFO estimation metric I gives a better IFO detection probability than that of the REA method, which is proved by simulations in Section 4.

To remove the channel effect from (11), we divide the $R(\tilde{\varepsilon}_I)$ with $R(\tilde{\varepsilon}_I + 1)$, and we get the following:

$$\frac{R(\tilde{\varepsilon}_I)}{R(\tilde{\varepsilon}_I + 1)} = e^{j\pi/N} \frac{\sin\{\pi(\tilde{\varepsilon}_I - \varepsilon)/N\}}{\sin\{\pi(\tilde{\varepsilon}_I - \varepsilon + 1)/N\}}. \tag{16}$$

Since $e^{j\pi/N}$ is a constant for given N, (16) is depend only on $\sin\{\pi(\tilde{\varepsilon}_I - \varepsilon)/N\} / \sin\{\pi(\tilde{\varepsilon}_I - \varepsilon - 1)/N\}$, which is negative when $\tilde{\varepsilon}_I < \varepsilon < \tilde{\varepsilon}_I + 1$. In OFDM systems, generally $N \gg 1$, and hence

$$\angle\left\{\frac{R(\tilde{\varepsilon}_I)}{R(\tilde{\varepsilon}_I + 1)}\right\} \approx \begin{cases} \pi, & \tilde{\varepsilon}_I < \varepsilon < \tilde{\varepsilon}_I + 1 \\ 0, & \text{otherwise,} \end{cases} \tag{17}$$

where $\angle\{\cdot\}$ denotes the argument of a complex number.

Similarly,

$$\angle\left\{\frac{R(\tilde{\varepsilon}_I)}{R(\tilde{\varepsilon}_I - 1)}\right\} \approx \begin{cases} \pi, & \tilde{\varepsilon}_I - 1 < \varepsilon < \tilde{\varepsilon}_I \\ 0, & \text{otherwise.} \end{cases} \tag{18}$$

Using characteristics of (17) and (18), we propose the second IFO estimator, which is represented with a pseudocode as below.

$\hat{\varepsilon}_\mathrm{t} = \arg\max_{\tilde{\varepsilon}_I} |R(\tilde{\varepsilon}_I)|^2$

if $|\angle\{R(\hat{\varepsilon}_\mathrm{t})/R(\hat{\varepsilon}_\mathrm{t} - 1)\}| \leq |\angle\{R(\hat{\varepsilon}_\mathrm{t})/R(\hat{\varepsilon}_\mathrm{t} + 1)\}|$

$\hat{\varepsilon}_I = \hat{\varepsilon}_\mathrm{t}$

else

$\hat{\varepsilon}_I = \hat{\varepsilon}_\mathrm{t} - 1$

end

4. SIMULATION RESULTS

4.1 Simulation Parameters

Simulation results have been obtained under the following conditions. The symbols X_k in (1) are QPSK modulated sequence and the FFT size N is 64. A cyclic prefix (CP) of 8 samples is used.

In these simulations, two channel models are considered: AWGN and four-path Rayleigh fading channels. In Rayleigh fading channel model, the four paths have delays of 0, 2, 4, and 6 samples, respectively. The amplitude A_l of the lth path is varies independently from the others according to a Rayleigh distribution with exponential power delay profile, and the power ratio of the first and last tap is set to be 20 dB., i.e., $E\{A_l^2\} = \exp(-0.8l)$. The Doppler bandwidth of 0.025 (corresponding to a mobile speed of 135 km/h) and a carrier frequency of 1 GHz are assumed. All simulation results were obtained with 2×10^4 iterations for AWGN channel and 3×10^4 iterations for Rayleigh fading channel.

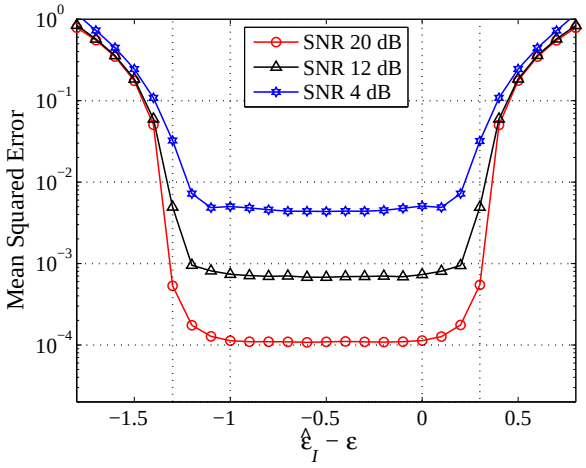

Figure 5: Mean squared error of frequency offset estimate according to $\varepsilon - \varepsilon_I$ (AWGN channel).

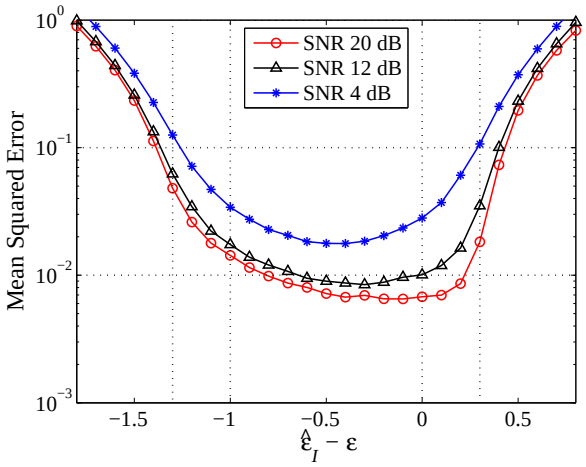

Figure 6: Mean squared error of frequency offset estimate according to $\varepsilon - \varepsilon_I$ (fading channel).

4.2 Simulation Results

Figs. 5 and 6 show the mean squared error (MSE) of final estimate according to $\hat{\varepsilon}_I - \varepsilon$ in the AWGN channel and Rayleigh fading channel, respectively. As we can see from the figure, the best performances are obtained from the region $\hat{\varepsilon}_I - \varepsilon \in [-1, 0]$ (in the case of SD), and performance degradation occurs in the other regions. This is because detection in SD region gives two successive estimation chances, as mentioned in Section 3.

In Fig. 6, the results are not symmetric with respect to centroid of the figure, whereas the results in Fig. 5 are symmetric. This is because that the FFO estimation metric (9) and RFO estimation metric (10) exploit the symmetric property of (8), and in the AWGN channel, the symmetry is conserved. However, in the multipath channel, the (8) can lose the symmetry due to multipath.

Figs. 7 and 8 show the IFO detection probabilities according to signal to noise ratio (SNR) in the AWGN and Rayleigh fading channels, respectively, when ε_F is 0.1. In the figures, we displayed two IFO detection probabilities; SD and total detection probabilities. The SD and SD+TD denote strict detection probabilities and total

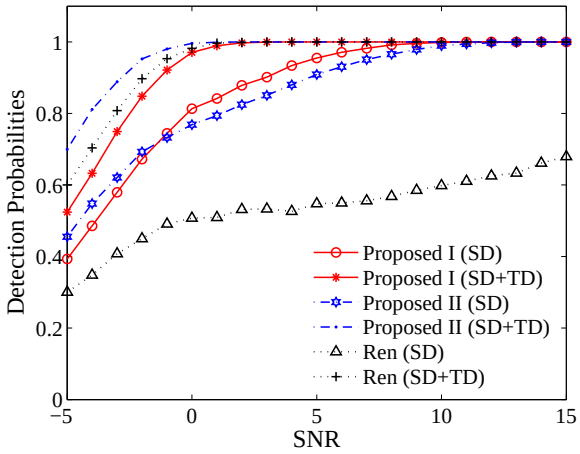

Figure 7: IFO detection probabilities according to SNR in the AWGN channel with $\varepsilon_F = 0.1$.

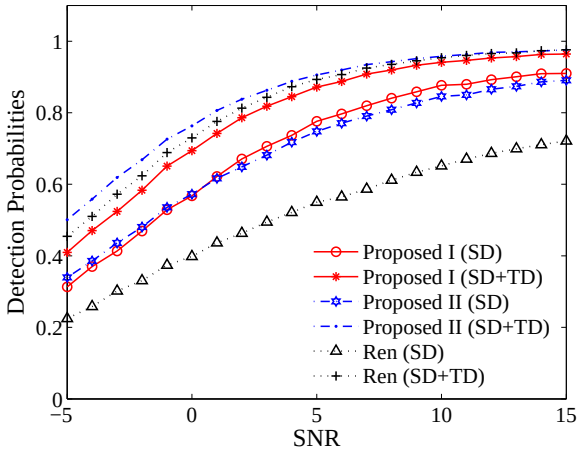

Figure 8: IFO detection probabilities according to SNR in the fading channel with $\varepsilon_F = 0.1$.

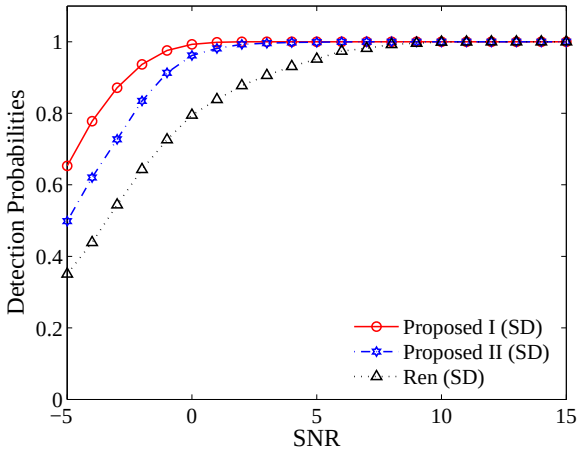

Figure 9: IFO detection probabilities according to SNR in the AWGN channel with $\varepsilon_F = 0.35$.

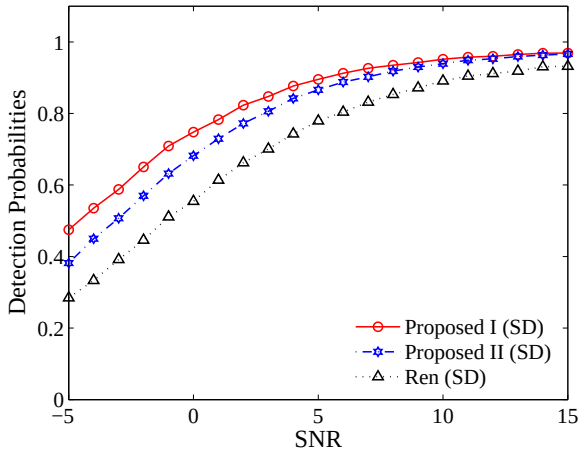

Figure 10: IFO detection probabilities according to SNR in the fading channel with $\varepsilon_F = 0.35$.

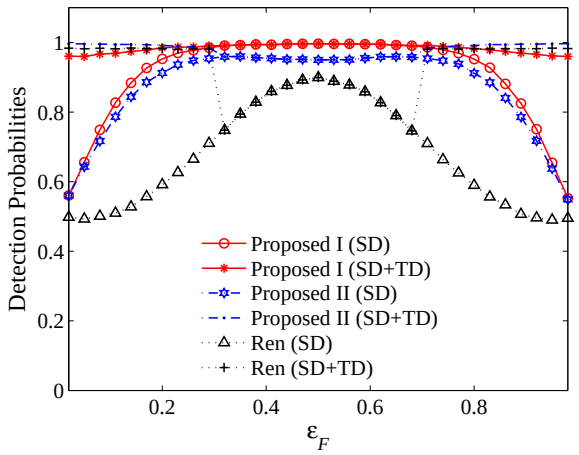

Figure 11: IFO detection probabilities according to ε_F in the AWGN channel with SNR 0 dB.

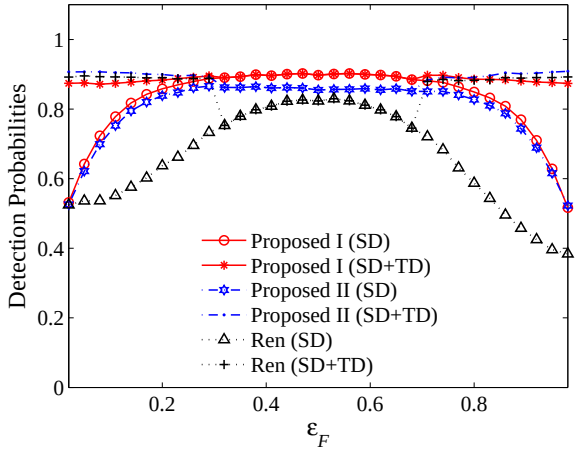

Figure 12: IFO detection probabilities according to ε_F in the fading channel with SNR 5 dB.

detection probabilities, respectively. We can see that the proposed II has the best performance in view of total detection probabilities, whereas the proposed I has good performance in view of SD probabilities. As mentioned in Section 3, since the SD gives more accurate results than TD in final estimates, the SD probability is one of the important performance measures.

Figs. 9 and 10 show the IFO detection probabilities according to SNR in the AWGN and Rayleigh fading channels, respectively when ε_F is 0.35. In the case of $\varepsilon \in (0.31, 0.69)$, TD cannot be defined, and therefore, the SD probabilities are considered only. As we can see from the figure, the proposed methods I and II outperform the REA method in terms of the SD probabilities.

Figs. 11 and 12 show the IFO detection probabilities according to ε_F in the AWGN channel with SNR 0 dB and Rayleigh fading channel with SNR 5 dB, respectively. In the case of $\varepsilon_F \in [0.31, 0.69]$, the REA method has poor detection probabilities, which is because the REA IFO estimation metric (7) has large values at the outside of detection range, as mentioned in Section 3. However, the proposed methods I and II still have a good detection probabilities in the range of $\varepsilon_F \in (0.31, 0.69)$. Consequently, the proposed methods are more robust to distribution of ε_F than the REA method.

5. CONCLUSION

In this paper, we first have analyzed REA frequency offset estimation method, and have found out that the detection probability of IFO is varying according to FFO. Thereafter, we have defined new detection criteria suitable for OFDM IFO detection, and proposed two novel IFO detection methods based on the ML principle and new detection criteria. The proposed methods still have the advantage that can be estimated independently from the structure of training symbol like the REA method. Moreover, the proposed methods overcome the problem of REA method and give better IFO detection probabilities compared to the REA method.

6. ACKNOWLEDGMENTS

This work was supported by the Korea Research Foundation Grant funded by the Korean Government (MOEHRD, Basic Research Promotion Fund) (KRF-2007-331-D00295).

The authors would like to thank anonymous reviewers for their valuable comments that improved this paper.

7. REFERENCES

[1] R. V. Nee and R. Prasad, *OFDM for Wireless Multimedia Communications*. London, England: Artech House, 2000.

[2] M. Morelli, C.-C. J. Kuo, and M. O. Pun, "Synchronization techniques for orthogonal frequency division multiple access (OFDMA): A tutorial review," *Proc. IEEE*, vol. 95, pp. 1394-1427, July 2007.

[3] K. Fazel and S. Kaiser, *Multi-Carrier and Spread Spectrum Systems*. West Sussex, England: John Wiley and Sons, 2003.

[4] P. H. Moose, "A technique for orthogonal frequency division multiplexing frequency offset correction," *IEEE Trans. Commun.*, vol. 42, pp. 2908-2914, Oct. 1994.

[5] T. M. Schmidl and D. C. Cox, "Robust frequency and timing synchronization for OFDM," *IEEE Trans. Commun.*, vol. 45, pp. 1613-1621, Dec. 1997.

[6] M. Morelli and U. Mengali, "An improved frequency offset estimator for OFDM applications," *IEEE Commun. Lett.*, vol. 3, pp. 75-77, Mar. 1999.

[7] Y. H. Kim, I. Song, S. Yoon and S. R. Park, "An efficient frequency offset estimator for OFDM systems and its performance characteristics," *IEEE Trans. Vehic. Technol.*, vol. 50, pp. 1307-1312, Sep. 2001.

[8] A. Laourine, A. Stéphenne, and S. Affes, "A new OFDM synchronization symbol for carrier frequency offset estimation," *IEEE Signal Process. Lett.*, vol. 14, pp. 321-324, May 2007.

[9] G. Ren, Y. Chang, H. Zhang, and H. Zhang, "An efficient frequency offset estimation method with a large range for wireless OFDM systems," *IEEE Trans. Vehic. Technol.*, vol. 56, pp. 1892-1895, July 2007.

[10] S. M. Kay, *Fundamentals of Statistical Signal Processing: Estimation Theory*. Englewood Cliffs, NJ: Prentice-Hall, 1993.

[11] S. M. Kay, *Fundamentals of Statistical Signal Processing: Detection Theory.* Englewood Cliffs, NJ: Prentice-Hall, 1998.

[12] V. M. Baronkin, Y. V. Zakharov, and T. C. Tozer, "Maximum likelihood single tone frequency estimation in a multipath channel," *IEE Proc. Commun.*, vol. 148, pp. 400-404, Dec. 2001.